


RESEARCH

Open Access



Performance analysis of a novel ejector-assisted condenser outlet split dual-evaporator refrigeration system

Gulshan Sachdeva¹, Parinam Anuradha², Vaibhav Jain^{3*}  and Y. T. VenkataTeja¹

Abstract

The performance of an ejector-assisted condenser outlet split dual-evaporator cycle is compared with a conventional dual-evaporator cycle albeit consisting a pressure reducing valve. The cycles do not employ any separator due to its inability to efficiently separate the liquid and the vapor phases. The comparison of both the cycles has been made for the same cooling capacity in low-temperature evaporator and unit flow rate of R134a and R1234yf as refrigerants. The impacts of changing the operating temperatures of evaporator and condenser have been examined in the current investigation. The study reveals that with the increase in temperature of the high-temperature evaporator, the cooling capacity of the high-temperature evaporator yields, while that of the low-temperature evaporator plummets in both the cycles. Further, the compressor work is allayed in the ejector-assisted cycle; thus, the COP is enhanced considerably. The percentage COP improvement over the basic cycle is obtained from 14.7 to 17.53% for the refrigerant R1234yf and from 14.45 to 17.32% for R134a; however, the COP of both the cycles with R1234yf is slightly lower than with R134a. The ejector has been modeled assuming a constant pressure theory. The observed trend indicates that the entrainment ratio is improved with the rise in the temperature of low-temperature evaporator, whereas it is decreased with the rise in the temperature of high-temperature evaporator.

Keywords Condenser outlet split, Dual evaporator, Ejector, COP, Entrainment ratio

1 Introduction

The global demand for HVAC&R systems has been experiencing an exponential growth. Consequently, the surge in demand has been exerting increasing pressure on power plants to consume larger amounts of fossil fuels to meet the energy requirements of these systems. The excessive burning of fuel is having catastrophic effects on our environment. Thus, there is a need to improve the performance of these energy guzzlers to reduce the load on the power plants. Another issue with these cooling

devices is the use of synthetic refrigerants which have been held responsible for global warming and depletion of the ozone layer. As a result, researchers are dedicating their efforts towards discovering environmentally friendly refrigerants with zero GWP and ODP. Most of the commercialized cooling systems work on the vapor compression cycle (VCC). In a VCC, condensed refrigerant at high pressure is expanded in an expansion device like capillary tube and expansion valve. This expansion or throttling process is irreversible in nature and thus responsible for energy loss. It has been established that an ejector, if used for the expansion, can reduce this loss. The expansion in the ejector is isentropic which is reversible and thus reduces throttling loss. Moreover, it recovers some of the energy lost in expansion and thus reduces compressor work. In a two-phase ejector, the refrigerant changes from liquid to mixed phase after expanding in

*Correspondence:

Vaibhav Jain

vaibhavursaathi@gmail.com

¹ National Institute of Technology, Kurukshetra, Haryana, India

² U.I.E.T., Kurukshetra University, Thanesar, India

³ Maharaja Agrasen Institute of Technology, Delhi, India

the nozzle of the ejector, whereas the ejector used in a heat-assisted cooling system deals with the vapor phase only, so that is known as a single-phase ejector. Kornhauser [1] first of all found the COP improvement of 21% with the ejector-assisted vapor compression cycle (EA-VCC) over the conventional VCC. The performance of system was evaluated with R12. J. Sarkar [2, 3] analyzed a single evaporator VCC assisted with an ejector and a separator for the natural refrigerants, ammonia, isobutene, and propane. The maximum COP enhancement of 26.1% with propane was obtained. Li et al. [4] investigated the same configuration for a new refrigerant R1234yf and concluded that the improvement was prominent at high condenser and low evaporator temperatures. Considerable research has been reported on single evaporator VCC with ejector as the expansion device.

Modern refrigerating equipments have two evaporators: one is used for the food section and the other for the freezer section. The freezer section operates at a lower temperature than the food section. In a single evaporator system, the air circulation rate within the food compartment is generally lower, leading to a significant temperature fluctuation. Moreover, operating the system at a lower temperature, i.e., freezer temperature, decreases the humidity of air flowing in the food compartment. With an individual evaporator in each compartment, humidity and air flow rate can be maintained easily. The energy saving can also be achieved through a dual-evaporator system, given that refrigerating the food compartment necessitates an elevated evaporator temperature compared to the freezer compartment. Gan et al. [5] determined the energy saving of 30% while using two separate VCCs with mechanical subcooling and suction line heat exchanger for freezer and food compartments compared to a single VCC operating at the freezer temperature for the same refrigeration capacity. A novel configuration of VCC with separation after condenser and having a sub-cooler and another condenser was proposed by Yan et al. [6] for a zeotropic mixture R290/R600a. The partially condensed refrigerant was separated into liquid and vapor phase. The liquid composition with R600a on the higher side was subcooled in a sub-cooler and produced cooling effect in the food section. With this configuration, the average COP improvement of 3.68% was achieved.

The ejector has also been used in the VCC developed for dual evaporator, and these studies reveal that the ejector is capable to enhance the performance of a dual-evaporator VCC. Hadi et al. [7] represented a system wherein a grouping of ejector, separator, and expansion valve were used to produce cooling in the evaporators. Instead of using pressure reducing valve, a pair of compressors were utilized to manage the output from the two evaporators

operating at distinct pressures. The COP enhancement of 48% was reported in the proposed cycle. A novel dual-evaporator ejector-assisted compression configuration with a separator was studied by Cui et al. [8]. Cui et al. [9] executed a novel experimental work pertaining to COS cycle employing an adjustable area ejector as a substitute of pressure reducing valve after high-pressure evaporator. The system efficiency got improved because of pressure recovery in the ejector and reduced load across the compressor. Multievacuator ejector-assisted vapor compression system with a separator was examined by Sarkar [10] for a transcritical fluid, i.e., CO₂. In the condenser split configuration, an ejector was used between the evaporators instead of a pressure regulating valve. However, the author separated the mixed refrigerant after the ejector and supplied the liquid part to the low-temperature evaporator after expanding in a conventional expansion device. Second configuration was not a condenser split. Sarkar [10] rather used a flooded evaporator and then separated the liquid and vapor part. The liquid fraction underwent expansion and was directed into the second evaporator. The rest of the configuration was same as the first arrangement. It was noticed that both the cycles performed better when the cooling duty across the evaporators was increased. These cycles assumed a perfect vapor–liquid separator, and it was found that the separator inefficiency can make the two-phase ejector no longer beneficial.

Lawrence and Elbel [11] experimentally tested the single evaporator vapor compression cycle, condenser outlet split dual-evaporator cycle, and ejector outlet split (EOS) dual-evaporator cycle using ejector for R134a and R1234yf refrigerants. The outcome was focused on the effect of the variation of the entrainment ratio. The authors [11] extended their work [12] on the same configuration but to analyze the effect of compressor oil return, poor ejector performance, and splitting of the two-phase flow. They further extended their work [13] to understand the work recovery rate with the entrainment ratio at three different compressor speeds. Latra et al. [14] mainly focused at single evaporator ejector-assisted vapor compression system and examined the effect of ejector area ratio and Mach number in the mixing section of the ejector. They briefly discussed the same configuration as in the present paper for the COP improvement only. At condenser temperature of 40 °C, improvement of COP obtained was more than 17% for both refrigerants. The enhancement in COP was greater for R1234yf, particularly at higher condenser temperatures. Unal and Yilmaz [15] reported COS system using ejector with R134a as refrigerant, and the effects of subcooling, condenser, and evaporator temperature were highlighted for the air-conditioning of buses. An increase

in the degree of subcooling considerably decreased the entrainment ratio but increased the COP. Unal [16] determined the dimensions of ejector used in COS cycle for R134a. Joen et al. [17] assessed the impacts of geometry of the ejector in a COS cycle, which was utilized in a household refrigerator-freezer equipped with R600a refrigerant. Joen et al. [18] also conducted a comparative analysis between a dual-evaporator system and an equivalent single evaporator system. Gao et al. [19] conducted a numerical comparison of COS ejector cycle and proposed a configuration that featured a combination of a flooded and dry evaporator. The results depicted 10% improvement of COP over the COS ejector cycle while working with R290.

R1234yf has thermodynamic properties that are very close to R134a, and thus, it is being considered as a possible alternative for R134a in the refrigeration systems. Zilio et al. [20] conducted experiments to specify minor and major modifications required in the air conditioning system working with R134a while replacing it with a potential alternative R1234yf and found it a potential alternative. A similar configuration was analyzed by Kim et al. [21] but to find the effects of nozzle throat diameter on the performance.

Many studies on the different configurations of bi-evaporator cooling systems based on conventional vapor compression technology are available in the open literature. However, limited research has been carried out using ejectors in the vapor compression system. After extensively reviewing the literature, it is concluded that only a few research papers can be obtained on

dual-evaporator refrigeration systems wherein the ejector has been used as an expansion device without a separator. The existing studies without separator are focused on the ejector parameters and have not compared the cycle with the conventional one. The aim of this analysis is to assess the performance of a dual-evaporator cycle that incorporates an ejector but without any separator. A comparative assessment has been conducted between R134a and R1234yf, identified as the most appropriate alternative to R134a. The analysis compares COS ejector cycle and COS conventional cycle for the similar working parameters. The modelling of the ejector is done using constant pressure mixing methodology, and the performance is analyzed for condenser and evaporator temperatures with unit mass flow rate condition.

2 Cycle description

Figure 1 depicts a schematic of the ejector-assisted dual-evaporator cycle (EA-DEC) along with its P-h curve. The proposed configuration includes a condenser, compressor, expansion valve, two-phase ejector, and two evaporators at unlike operating temperatures. The condensed refrigerant at state 3 is separated in two different parts. One of the parts undergoes expansion from state points 3 to 4, maintaining constant enthalpy, through an expansion valve and takes cooling load of evaporator-2 (low temperature). The dry saturated vapor leaving evaporator at state 5 is named secondary fluid.

Other part of the condensed refrigerant, known as primary fluid, experiences expansion in motive nozzle section of the ejector and achieves state corresponding

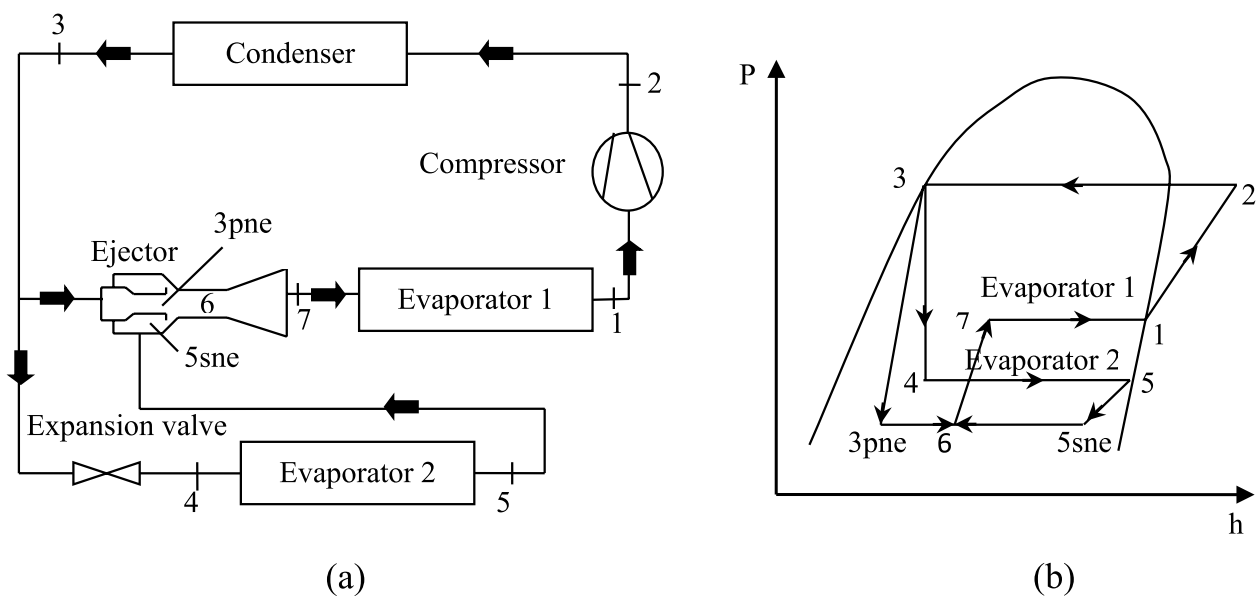
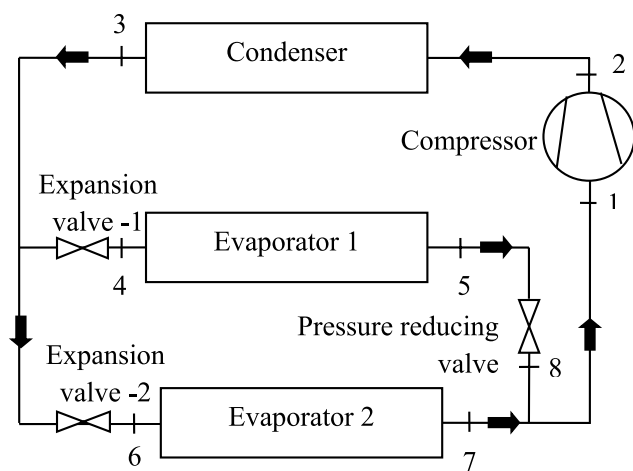


Fig. 1 a Configuration layout. b P-h diagram of EA-DEC

to $3p_{ne}$. The pressure at state $3p_{ne}$ is less than that in evaporator-2. Therefore, the ejector entrains the secondary fluid and expands it up to the state point $5s_{ne}$. The pressure after expansion of primary and secondary fluid is assumed same, and the constant pressure-mixing methodology is considered in the analysis. The mixed fluid is shown at state 6 in the P–h diagram. The process 6–7 is the isentropic compression that happens in the diverging section. The dry vapor is drawn by the compressor at state 1 after taking cooling load of evaporator-1. The isentropic compression performed by the compressor elevates the refrigerant's pressure to match the condenser pressure. The process 2–3 is the condensation process that happens in the condenser and the thermodynamic cycle continues.

Figure 2 illustrates a representation of conventional dual-evaporator cycle (C-DEC) along with its P–h diagram. It is a condenser outlet split dual-evaporator cycle. The condensed saturated liquid (state 3) is split and expanded in expansion valve-1 (state point 4). The refrigerant then takes refrigeration load in the evaporator-1. The other stream takes refrigeration load of the evaporator-2 after expansion. The dry saturated vapor exiting from the evaporator-1 is passed through a pressure-reducing valve to drop its pressure equal to the pressure of evaporator-2. Thereafter, a compressor compresses the mixed streams up to the condenser pressure. The process 2–3 is the condensation that happens in the condenser, and the thermodynamic cycle continues.



(a)

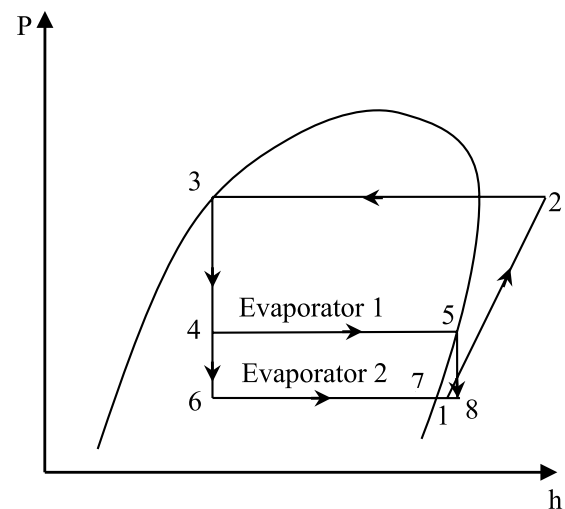
3 Assumptions and methodology

The modelling of both the cycles is done according to the following assumptions:

- The system works at steady-state conditions.
- The refrigerant exiting the condenser and evaporator is saturated.
- Pressure losses in the condenser, evaporator, and piping are inconsequential.
- Pressures at primary nozzle exit and secondary nozzle exit are the same.
- Constant pressure theory is applied for the mixing process.
- Kinetic energy of flow at the inlet and outlet of the ejector is negligible.
- The flow within the ejector is assumed as adiabatic and one-dimensional.
- The ejectors considered in the present work are not of known area ratio and entrainment ratio; instead for every operating condition, the ejector is optimized in terms of area ratio and entrainment ratio considering constant primary nozzle, secondary nozzle, and mixing efficiencies. It is assumed that for every change in the condenser or evaporator temperature, the ejector is designed to provide the same efficiencies by suitably manipulating the ejector geometry and manufacturing conditions.

3.1 Thermodynamic analysis

Mass, momentum, and energy have been conserved in all the components of cycles.



(b)

Fig. 2 a Configuration layout. b P–h diagram of C-DEC

Primary nozzle is as follows:

Primary nozzle efficiency

$$\eta_{pn} = \frac{h_3 - h_{3pne}}{h_3 - h_{3pne,is}} \quad (1)$$

$$h_{3pne,is} = f(p_{3pne}, s_3) \quad (2)$$

By solving Eq. 1, the enthalpy at primary nozzle exit is obtained.

Energy balance

$$h_3 = h_{3pne} + \frac{C_{3pne}^2}{2} \quad (3)$$

The velocity at the exit of the primary nozzle is determined through the solution of the aforementioned equation.

Area of primary nozzle at its exit:

$$a_{3pne} = \frac{m_p}{\rho_{3pne} C_{3pne}} \quad (4)$$

Secondary nozzle is as follows:

Secondary nozzle efficiency

$$\eta_{sn} = \frac{h_5 - h_{5sne}}{h_5 - h_{5sne,is}} \quad (5)$$

$$h_{5sne,is} = f(p_{5sne}, s_5) \quad (6)$$

The enthalpy at secondary nozzle exit is obtained by solving Eq. no. 5.

$$h_5 = h_{5sne} + \frac{C_{5sne}^2}{2} \quad (7)$$

The velocity at secondary nozzle exit is computed by the above equation.

Area of secondary nozzle at its exit:

$$a_{5sne} = \frac{m_s}{\rho_{5sne} C_{5sne}} \quad (8)$$

The pressure drops between the evaporator-2, and the exit of either the primary or secondary nozzle is given as follows:

$$\Delta p = p_5 - p_{5sne} \quad (9)$$

Mixing section is as follows:

Mixing has been considered at the constant pressure, thus:

$$p_6 = p_{5sne} \quad (10)$$

Momentum balance

$$m C_6 = \sqrt{\eta_{mix}} (m_p C_{3pne} + m_s C_{5sne}) \quad (11)$$

Energy balance

$$m_p h_3 + m_s h_5 = m \left(h_6 + \frac{C_6^2}{2} \right) \quad (12)$$

Diffuser outlet is as follows:

$$h_7 = m_p h_3 + m_s h_5 \quad (13)$$

$$h_7 = h_6 + \frac{C_6^2}{2} \quad (14)$$

Diffuser efficiency is as follows:

$$\eta_d = \frac{h_{7,is} - h_6}{h_7 - h_6} \quad (15)$$

$$p_7 = f(h_{7,is}, s_6) \quad (16)$$

Compressor is as follows:

$$h_{2,is} = f(p_3, s_1) \quad (17)$$

$$h_2 = h_1 + \frac{(h_{2,is} - h_1)}{\eta_{comp}} \quad (18)$$

The isentropic efficiency of the compressor is obtained as follows [20]:

$$\eta_{comp} = 0.874 - 0.0135 \left(\frac{p_2}{p_1} \right) \quad (19)$$

$$W_{comp} = m(h_2 - h_1) \quad (20)$$

Evaporators and condenser are as follows:

$$Q_{e1} = m(h_1 - h_7) \quad (21)$$

$$Q_{e2} = m_s(h_5 - h_4) \quad (22)$$

$$Q_c = m(h_2 - h_3) \quad (23)$$

The pressure lift ratio can be defined as follows:

$$PLR = \frac{p_7}{p_5} \quad (24)$$

The ejector's area ratio is expressed as the ratio between the mixing area and the exit area of the primary nozzle.

$$\phi = (a_{3pne} + a_{5sne}) / a_{3pne} \quad (25)$$

Entrainment ratio

$$\mu = m_s / m_p \quad (26)$$

The quality of ejector exiting flow must satisfy the following equation.

$$x_7 = 1 / (1 + \mu) \quad (27)$$

For unit flow rate of the refrigerant,

$$m_p = 1 / (1 + \mu) \quad (28)$$

$$m_s = \mu / (1 + \mu) \quad (29)$$

The COP of the EA-DEC is evaluated as follows:

$$COP_{EA-DEC} = (Q_{e1} + Q_{e2}) / W_{comp} \quad (30)$$

Then the improvement in COP of EA-DEC over the C-DEC can be given as follows:

$$COP_{imp} = (COP_{EA-DEC} - COP_{C-DEC}) / COP_{C-DEC} \quad (31)$$

Figure 3 displays the flowchart outlining the simulation procedure for EA-DEC. The simulation is carried out for the variation in condenser temperature T_3 and temperatures of both evaporators T_1 and T_5 . The efficiencies in the various sections of the ejector depend on the operating conditions; however, to consider the effect on the efficiencies, the empirical relations in terms of condenser and evaporator pressures/temperatures are required. The efficiencies also got varied with different refrigerants. The ejector model requires the assumption of efficiencies of the motive nozzle, suction nozzle, and diffuser, and many researchers [2–4, 7, 9, 11, 13–15] have taken the efficiencies constant in their simulations. In the present simulation, the efficiencies of primary nozzle η_{pn} , secondary nozzle η_{sn} , mixing η_{mix} , and diffuser η_d sections of the ejector are considered constant as 85%, 85%, 95%, and 90%, respectively. The pressure drop in the ejector and the entrainment ratio are assumed first and then iterated to get the outlet pressure of ejector same as the pressure of evaporator-1.

The conventional dual-evaporator VCC is simulated using identical condenser and evaporator temperatures as obtained in EA-VCC. The mass flow rate of refrigerant and the cooling capacity of evaporator-2 are also taken same as obtained in EA-DEC under identical condenser and evaporator temperatures. The refrigerant flowing

into the evaporator-1 is expanded in a conventional expansion device in C-DEC unlike ejector in EA-DEC; thus, a difference in the cooling capacity of evaporator-1 is observed.

4 Model validation

The ejector of a single evaporator ejector-assisted vapor compression system needs to be designed for a two-phase fluid system wherein condensed liquid refrigerant enters the primary nozzle and saturated vapor refrigerant is entrained from the evaporator. The same is happening in the ejector of the present configuration even though it employs two evaporators. The present configuration is modified to a single evaporator cooling system to get the simulation results validated with [4]. This validation is conducted using refrigerant R1234yf at an evaporator temperature of 5 °C, with the condenser temperature which varies from 35 to 55 °C. The efficiencies of nozzle, mixing, and diffuser portions of ejector are taken similar to Li et al. [4]. It is noted from Fig. 4 that the COP values obtained from the current model are closely aligned with those reported by Li et al. [4]. Thus, the validation of model is confirmed.

The conventional dual-evaporator vapor compression simulation has also been validated with [19] for the refrigerant R290 for the similar conditions as [19]. The condenser temperature is varied from 35 to 55 °C. The refrigeration capacity and load ratio of system are kept same as Gao et al. [19]. Table 1 shows that the outcome of the present model is in synchronous with that of Gao et al. [19].

Ejector is the most complex component in the present configuration. To provide more confidence in the simulation results, the ejector modelling is validated with Bilir and Ersoy [22] to establish its accuracy. The entrainment ratio and the area ratio of the ejector are validated at 5 °C evaporator temperature and 40 °C condenser temperature for the refrigerant R134a. The results are found to be in good agreement as shown in Table 2.

5 Results and discussion

The EA-DEC is theoretically investigated using EES software with both the refrigerants R134a and R1234yf under the operating parameters as given in Table 3. Being environmentally friendly, the refrigerant R1234yf is a potential candidate to replace R134a. The heat transfer coefficient and the pressure drop with HFO-1234yf are lower than that of HFC-134a during condensation and evaporation, respectively. Differences in the properties of R134a and R1234yf, though not in large amounts like boiling, critical point, molecular weight, saturation and pressures/temperatures, are the reasons for the difference in performance. The configuration, operating parameters,

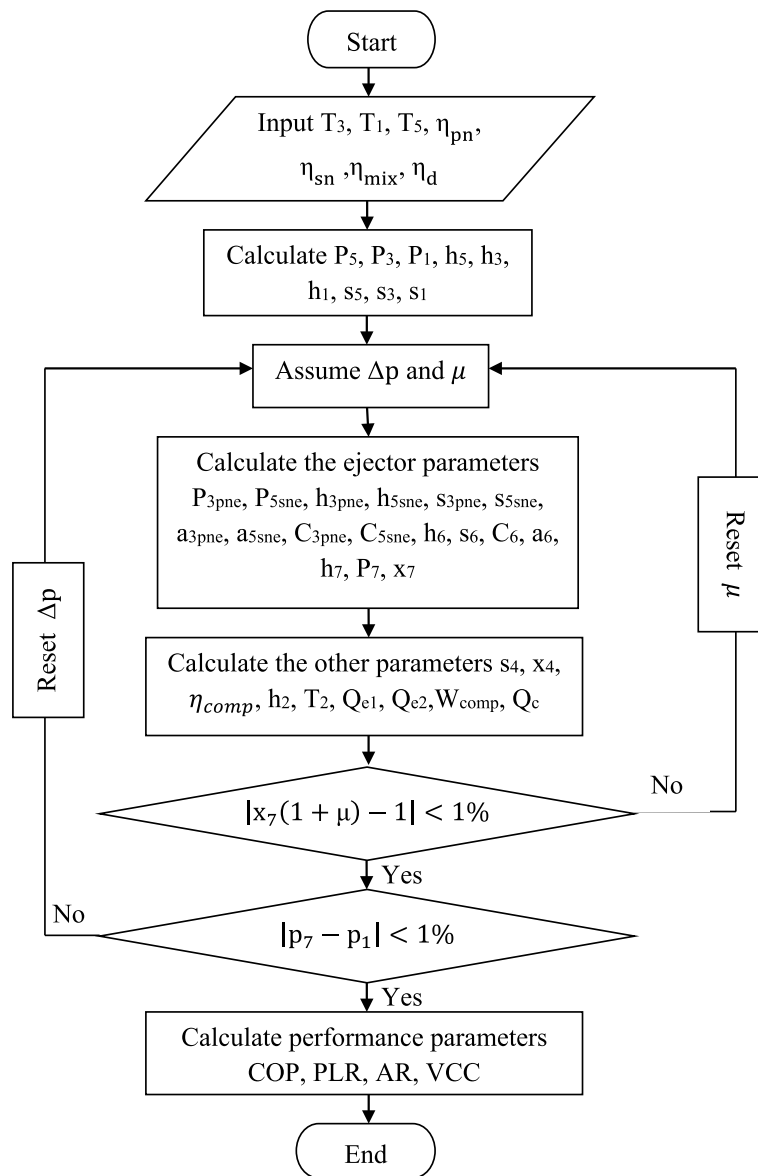


Fig. 3 Flow chart for simulation of EA-DEC

and efficiencies are considered same for both the working fluids. The yielded values of thermodynamic properties at various state points for R134a and R1234yf are presented in Table 4 and Table 5, respectively.

A comparative study of EA-DEC and C-DEC is performed for the same initial conditions. Further, the values of cooling duty and refrigerant flow of evaporator-2 calculated at the initial conditions for the EA-DEC are the additional inputs in the C-DEC. It is done to do the performance comparison for the same cooling capacity in evaporator-2. Table 6 shows that the cooling capacity obtained in the evaporator-1 of EA-DEC is slightly higher as compared to C-DEC. The dryness fraction

of the refrigerant at inlet of evaporator-1 of EA-DEC is more as compared to C-DEC, but the mass of refrigerant flowing in the evaporator-1 of EA-DEC is the total refrigerant of the system. The amount of liquid refrigerant in the evaporator-1 of EA-DEC is found to be higher which is the reason for slightly higher cooling capacity of the evaporator-1 for the conditions prescribed in Table 3. The compressor work required is less in EA-DEC due to suction at higher pressure than the C-DEC. The coefficient of performance of EA-DEC having R1234yf is 14.69% higher than the C-DEC. The COP is marginally higher with R134a, but the percentage improvement in COP is almost same for both the refrigerants.

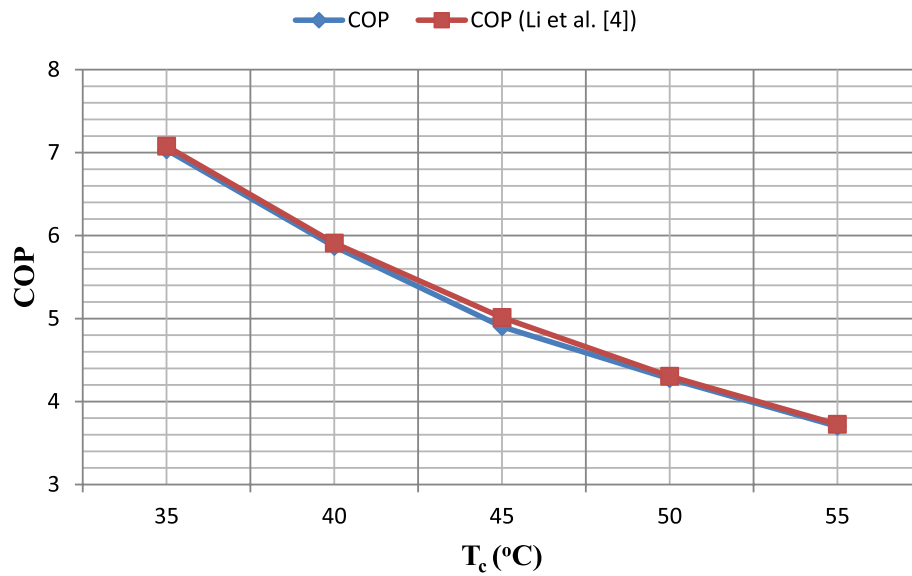


Fig. 4 Comparison of single evaporator ejector VCC and Li et al. [4]

Table 1 Validation of C-DEC with Gao et al. [19]

T _c (°C)	COP		
	Present C-DEC	Gao et al. [19]	Error (%)
35	6.876	6.86	0.23
40	5.709	5.7	0.15
45	4.845	4.838	0.14
50	4.182	4.175	0.16
55	3.657	3.65	0.19

Table 2 Ejector parameters validation with Bilir and Ersoy [22]

Parameter	Present analysis	Bilir and Ersoy [22]	Percent deviation (%)
Entrainment ratio	0.775	0.770	0.69
Area ratio	6.07	6.35	4.2

Table 3 Initial operating parameters

Input parameters	Values
Condenser temperature (T _c , °C)	45
Evaporator 1 temperature (T _{e1} , °C)	4
Evaporator 2 temperature (T _{e2} , °C)	0
Primary nozzle efficiency (η _{pn} , %)	85
Secondary nozzle efficiency (η _{sn} , %)	85
Diffuser efficiency (η _d , %)	90
Mixing section efficiency (η _{mix} , %)	95

Table 4 Thermophysical properties for R134a

State point	T (°C)	P (kPa)	m (kg/s)	h (kJ/kg)	s (kJ/kg-K)
1	4	337.9	1	252.8	0.9293
2	53.99	1161	1	283.7	0.9457
3	45	1161	1	115.8	0.4183
3pne	-3.742	255.3	0.5817	110.4	0.4219
4	0	293	0.4183	115.8	0.4385
5	0	293	0.4183	250.5	0.9314
5sne	-3.742	255.3	0.4183	248.1	0.9329
6	-3.742	255.3	1	168.3	0.6369
7	4	337.9	1	172.1	0.6383

Table 5 Thermophysical properties for R1234yf

State point	T (°C)	P (kPa)	m (kg/s)	h (kJ/kg)	s (kJ/kg-K)
1	4	360.9	1	365.8	1.598
2	45.77	1154	1	390.6	1.611
3	45	1154	1	261.1	1.206
3pne	-6.514	251.7	0.5992	255.6	1.21
4	0	315.8	0.4008	261.1	1.225
5	0	315.8	0.4008	363.2	1.598
5sne	-6.514	251.7	0.4008	359.8	1.6
6	-6.514	251.7	1	297.6	1.367
7	4	360.9	1	302.1	1.369

5.1 Effect of condenser temperature

Figure 5 depicts that the refrigeration capacity of both the evaporators decreases with the condenser

Table 6 Comparative results of EA-DEC and C-DEC

Parameter	R1234yf		R134a	
	EA-DEC	C-DEC	EA-DEC	C-DEC
Δp	64.1	-	37.7	-
PLR	1.143	-	1.153	-
μ	0.669	-	0.719	-
m_p (kg/s)	0.5992	0.5992	0.5817	0.5817
m_s (kg/s)	0.4008	0.4008	0.4183	0.4183
Dryness fraction at the inlet of evaporator-1	0.605	0.3514	0.5875	0.2994
Q_c (kJ/s)	129.5	131.8	167.9	171.2
Q_{e1} (kJ/s)	63.75	62.72	80.65	79.68
Q_{e2} (kJ/s)	40.92	40.92	56.32	56.32
Q_e (kJ/s)	104.7	103.64	137	136
W_{comp} (kJ/s)	24.78	28.14	30.97	35.19
COP	4.224	3.683	4.423	3.864

temperature rise of 35–45 °C for both the refrigerants and cycles. The refrigeration capacity variation of evaporator-2 is same for both the refrigerants and cycles, as these are designed this way only for the proper comparison of the cycles. The dryness fraction of the refrigerant after expansion increases with the rise in condenser temperature; thus, cooling capacity decreases. Total refrigeration capacity of both the cycles is almost same; however, the refrigeration capacity with refrigerant R1234yf is approximately

23.6% less than that obtained with R134a at 45 °C condenser temperature and unit flow rate of the refrigerants.

Figure 6 shows that the compressor power increases with the rise in condenser temperature. The compressor work required in EA-DEC with R134a and R1234yf remains lower than that of C-DEC for the same temperature rise in condenser, reason being the higher suction pressure in EA-DEC. It is found that the compressor work in EA-DEC working with R1234yf is 20% lower at 45 °C condenser temperature in comparison with R134a.

Figure 7 presents COP variation of EA-DEC with the condenser temperature. Increase in condenser temperature increases pressure load of the compressor, hence the compressor power, and expansion from the high condenser pressure lowers the cooling capacity; therefore, COP of both the cycles decreases for both the refrigerants with the rise in condenser temperature. The improvement in COP of EA-DEC over C-DEC is little higher with R1234yf in comparison to R134a for the considered range, though the COP of R134a is higher in both the cycles. The COP improvement is seen to reduce for both the refrigerants with the rise in condenser temperature, though the rate of reduction is less than as compared to COP. The COP improvement varies from 17.53 to 14.7% for the refrigerant R1234yf and from 17.32 to 14.45% for R134a.

Figure 8 highlights the change in entrainment ratio with the condenser temperature. The μ is bound to decrease with the rise in condenser temperature because of the

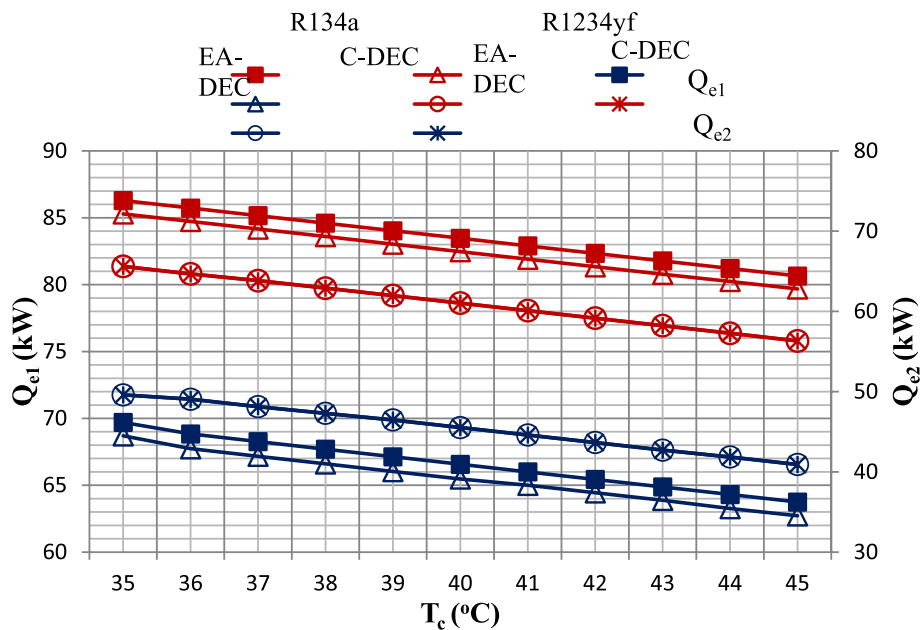


Fig. 5 Variation of refrigeration capacity with the condenser temperature

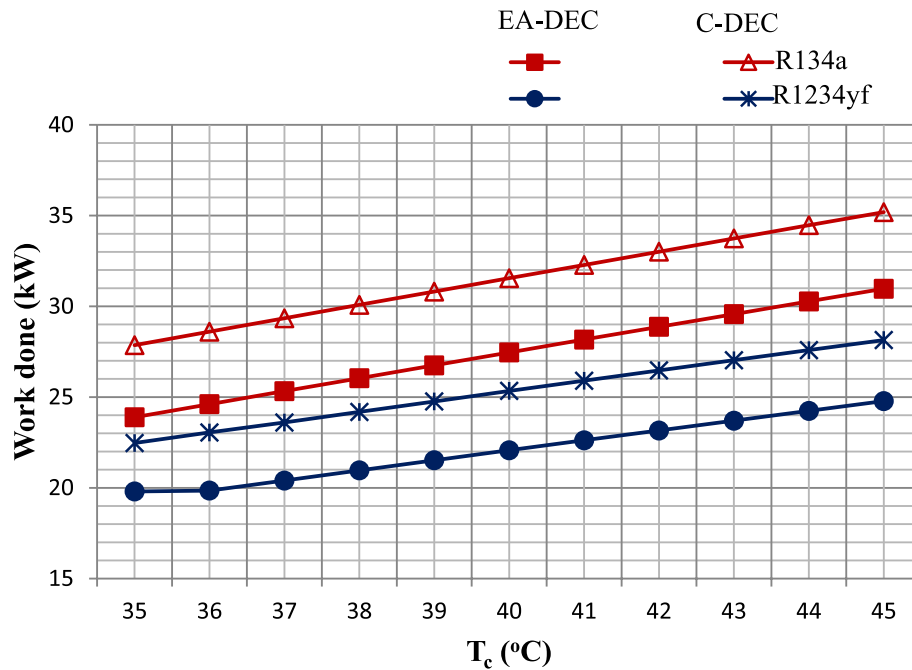


Fig. 6 Variation of compressor power with the condenser temperature

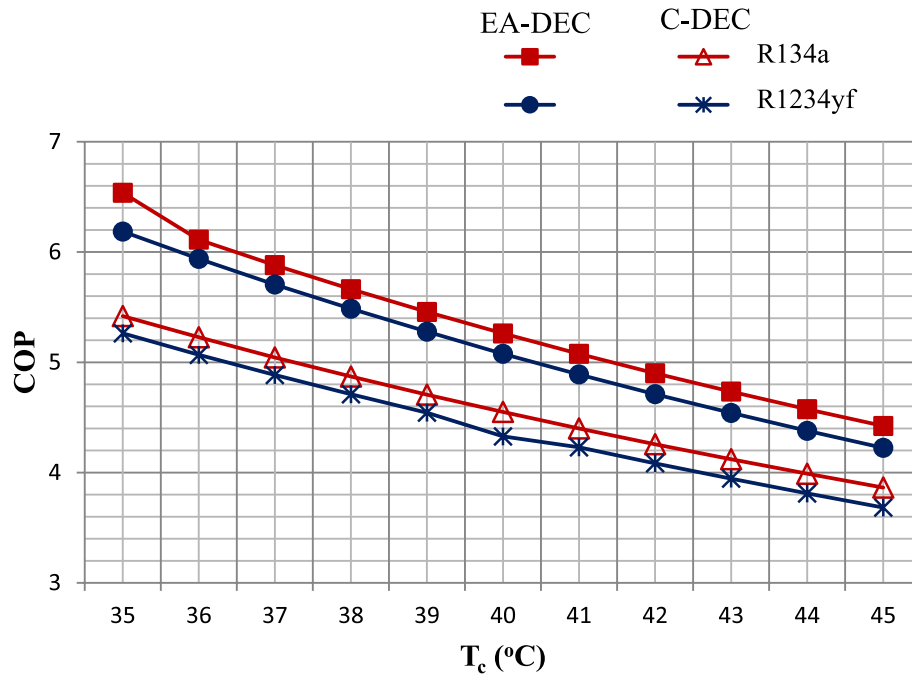


Fig. 7 Variation of COP variation along the condenser temperature

amplified primary refrigerant flow rate. The entrainment ratio varies between 0.781 and 0.719 for R134a, and it is between 0.748 and 0.669 for R1234yf.

5.2 Effect of evaporator-1 temperature

Figure 9 shows the refrigeration capacity variation of both the evaporators for the increase in evaporator-1 temperature from 4 to 14 °C while keeping the other conditions same as the initial input conditions. In EA-DEC,

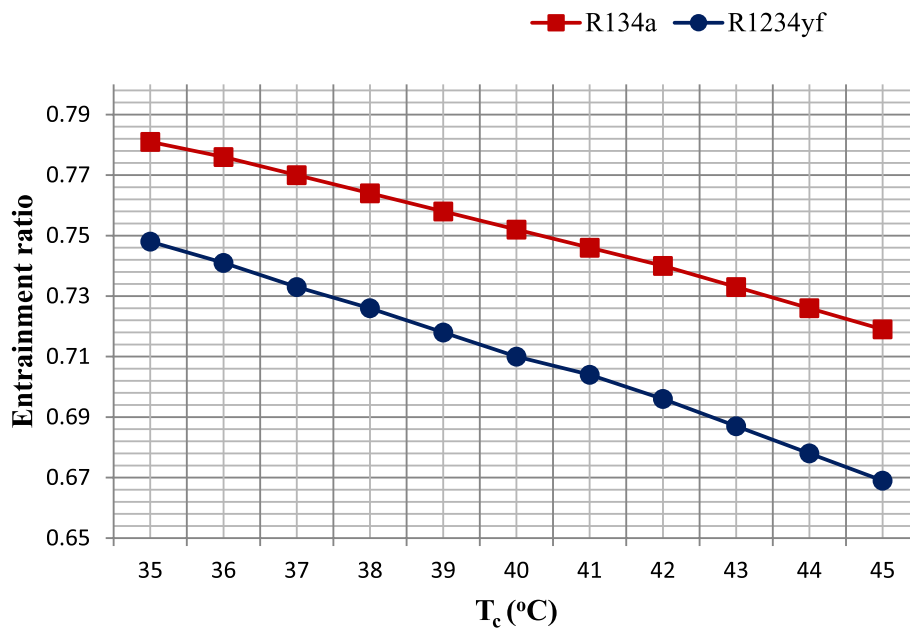


Fig. 8 Variation of entrainment ratio with the condenser temperature

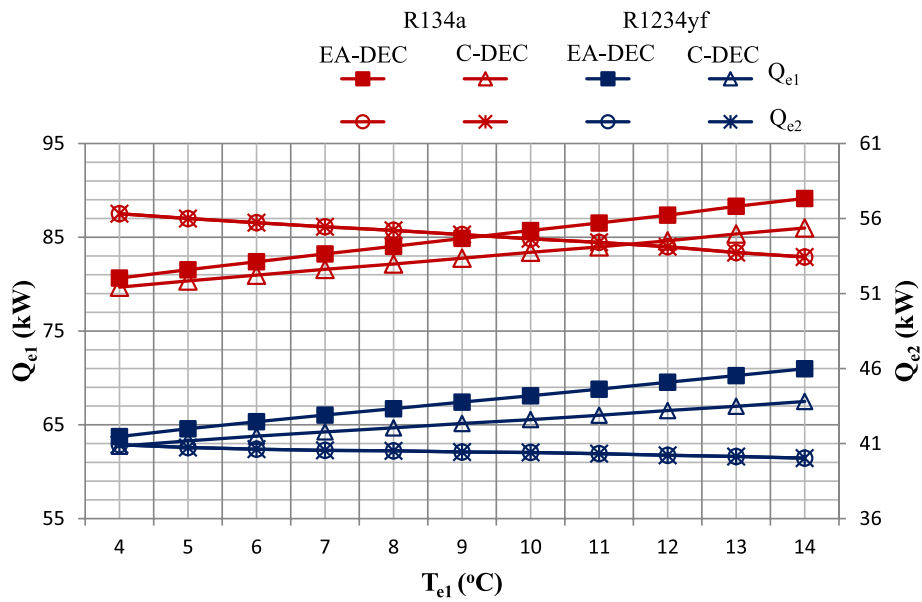


Fig. 9 Variation of cooling capacity with the evaporator-1 temperature

the primary refrigerant flow rate increases to meet the higher pressure demand at the ejector’s exit, and thus, the cooling duty of evaporator-1 increases. The increase in cooling duty is about 10.5 and 11.3% with R134a and R1234yf in EA-DEC, respectively. The dryness fraction varies from 0.5875 to 0.609 for R134a and from 0.605 to 0.614 for R1234yf. The secondary mass flow rate decreases, and thus, the cooling duty of evaporator-2

decreases. However, the decrease in cooling capacity is negligible with R1234yf, but it is 5.11% with R134a. The total refrigeration capacity increases in both the cycles; however, the increase is more in the EA-DEC.

Figure 10 depicts that the compressor power of EA-DEC decreases, and the reduction is 30% and 40% with the working fluids R1234yf and R134a, respectively, with the rise in evaporator-1 temperature from 4 to 14 °C.

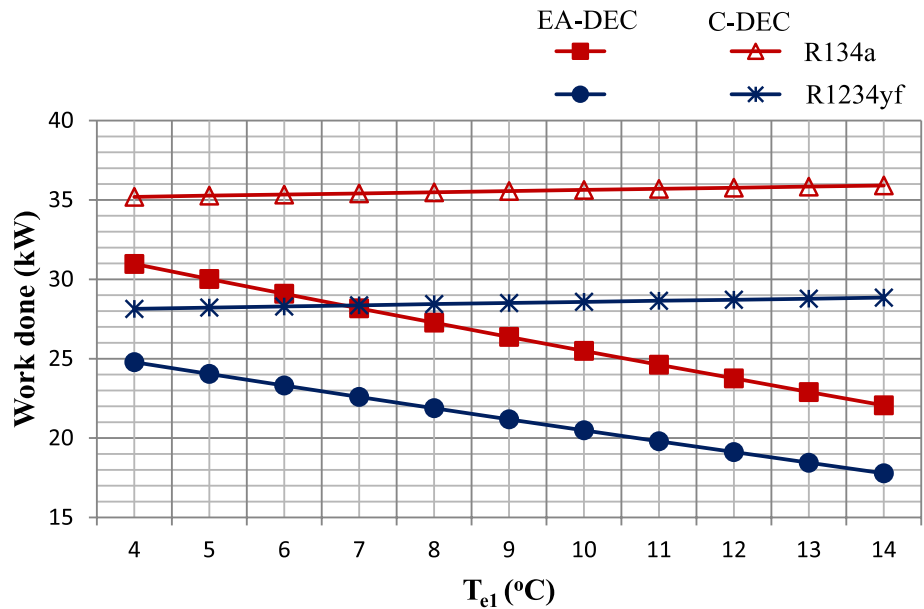


Fig. 10 Variation of compressor power with the evaporator-1 temperature

Increase in evaporator-1 temperature enhances the suction pressure of compressor and thus lowers its work. The suction pressure in case of C-DEC remains same as the pressure of evaporator-2; however, a small nudge in the compressor power is observed because of change in the mixing enthalpy at point 1.

Figure 11 depicts that the COP of EA-DEC increases at a very steep rate for both the refrigerants. As discussed,

cooling capacity increases, and compressor work reduces with the rise in evaporator-1 temperature; hence, COP increases. There is trivial effect on the COP of C-DEC. The improvement of COP of ejector-assisted cycle over the conventional cycle varies from 14.7 to 67.62% for R1234yf, and it is almost same for R134a.

Figure 12 depicts that the entrainment ratio reduces with the rise in evaporator-1 temperature. Rise in

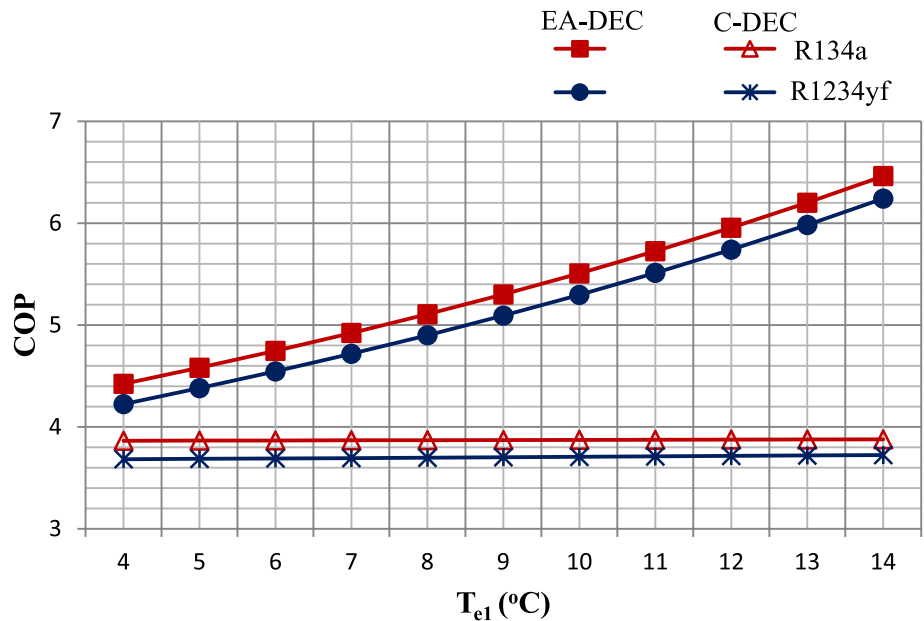


Fig. 11 Variation of COP with the evaporator-1 temperature

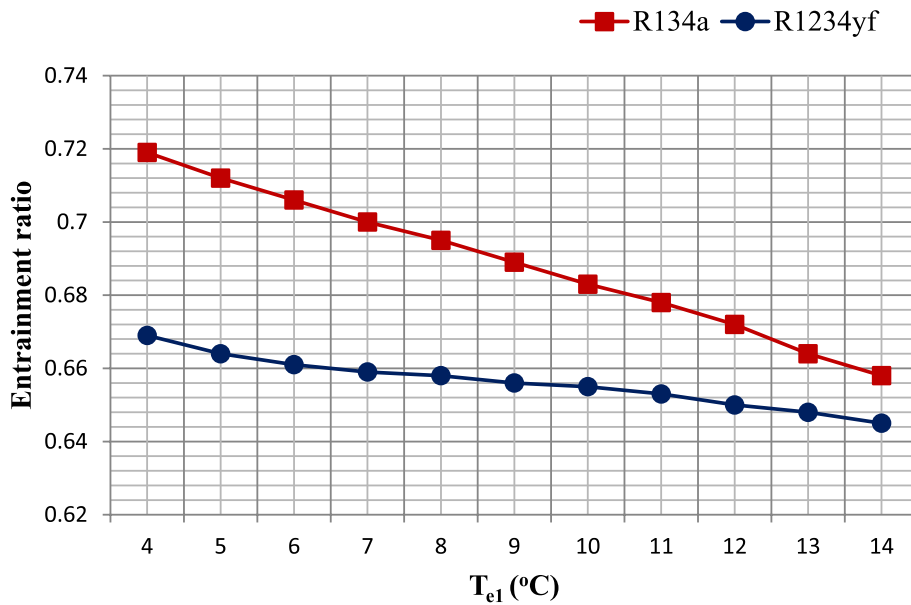


Fig. 12 Variation of entrainment ratio variation with evaporator-1 temperature

evaporator-1 temperature demands more pressure at the ejector exit, and thus, the primary refrigerant flow rate increases. It decreases entrainment ratio of the ejector. The entrainment ratio varies from 0.781 to 0.719 for R134a, and it is between 0.748 and 0.669 for R1234yf. The pressure lift ratio increases with the rise in evaporator-1 temperature.

5.3 Effect of evaporator-2 temperature

Figure 13 shows the variation of refrigeration capacity of EA-DEC and C-DEC with evaporator-2 temperature. In the EA-DEC, the primary refrigerant flow rate decreases to entrain the secondary fluid at high pressure, and thus, the cooling duty of evaporator-1 decreases. The reduction in the cooling capacity is about 5% and 3.6% with R134a and R1234yf in EA-DEC respectively. The dryness fraction varies between 0.5875–0.62 for R134a

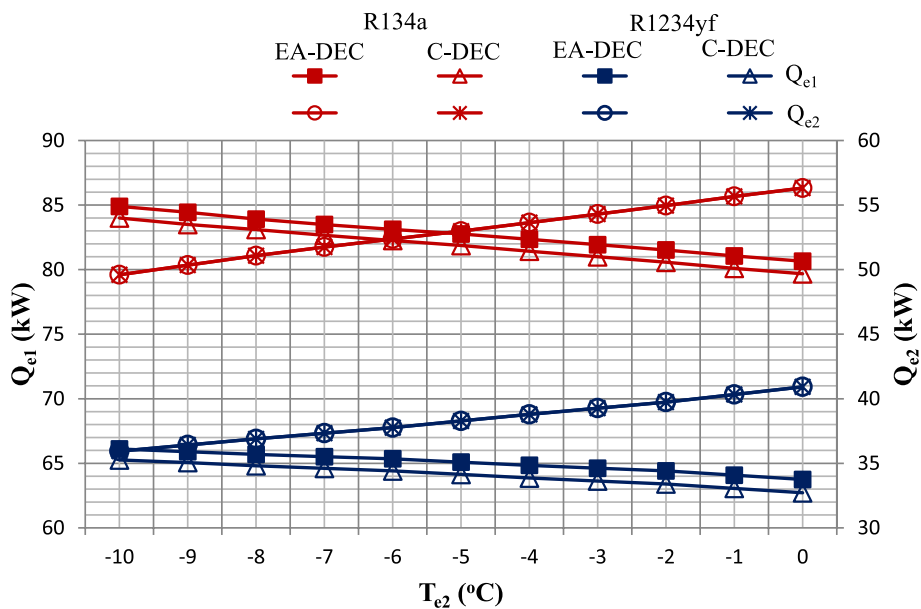


Fig. 13 Variation of cooling capacity with the evaporator-2 temperature

and 0.605–0.63 for R1234yf. It is to be noted that total amount of refrigerant flows in the evaporator-1 in case of EA-DEC. The secondary refrigerant flow rate increases, and thus, the cooling duty of evaporator-2 yields. The total refrigeration duty increases in both the cycles; however, the increase is more in the EA-DEC.

Figure 14 shows that with the increase in evaporator-2 temperature, compressor work decreases progressively in conventional cycle, but in contrast, there is no effect on compressor work of ejector-assisted cycle. In C-DEC, the suction pressure of compressor increases which in turn lowers the compressor work. However, the compressor work is still more as compared to EA-DEC for the considered temperature range. The compressor work decreases by 26% and 25% with R134a and R1234yf, respectively.

Figure 15 shows a considerable increase in COP in C-DEC with the increase in evaporator-2 temperature, reason being reduction in compressor power. The COP of EA-DEC remains almost constant; therefore, the improvement of COP decreases from 53.54 to 14.7% with R1234yf for the considered range of evaporator-2 temperature.

Figure 16 depicts that the entrainment ratio enhances with the rise in evaporator-2 temperature. Increase in evaporator-2 temperature provides secondary fluid at high pressure and thus decreases primary refrigerant flow rate. It increases entrainment ratio of the ejector. The entrainment ratio increases from 0.629–0.719 to 0.602–0.669 for R134a and R1234yf, respectively. The

pressure lift ratio gets lowered with the increase in evaporator-2 temperature. The PLR is more for R134a than R1234yf due to the refrigerant properties.

6 Conclusions

In present work, energy analysis of a COS cycle with no separator and two-phase ejector is examined for R134a and R1234yf refrigerants. The performance characteristics of EA-DEC with constant pressure mixing ejector model have been investigated. The study can be concluded as under the following:

1. The total refrigeration capacity enhances with the rise in condenser temperature; however, there is no difference in the values of total refrigeration capacity of ejector-assisted and conventional dual-evaporator cycle with the condenser temperature variation. The refrigeration capacity with refrigerant R1234yf is approximately 23.5% less than that obtained with R134a at 45 °C condenser temperature and unit flow rate of the refrigerants.
2. The COP improvement is found to decrease for both the refrigerants with the rise in condenser temperature due to increase in compressor work; however, rate of decrease is less than the rate of decrease of COP itself. The COP improvement varies from 17.53 to 14.7% for the refrigerant R1234yf and from 17.32 to 14.45% for R134a.

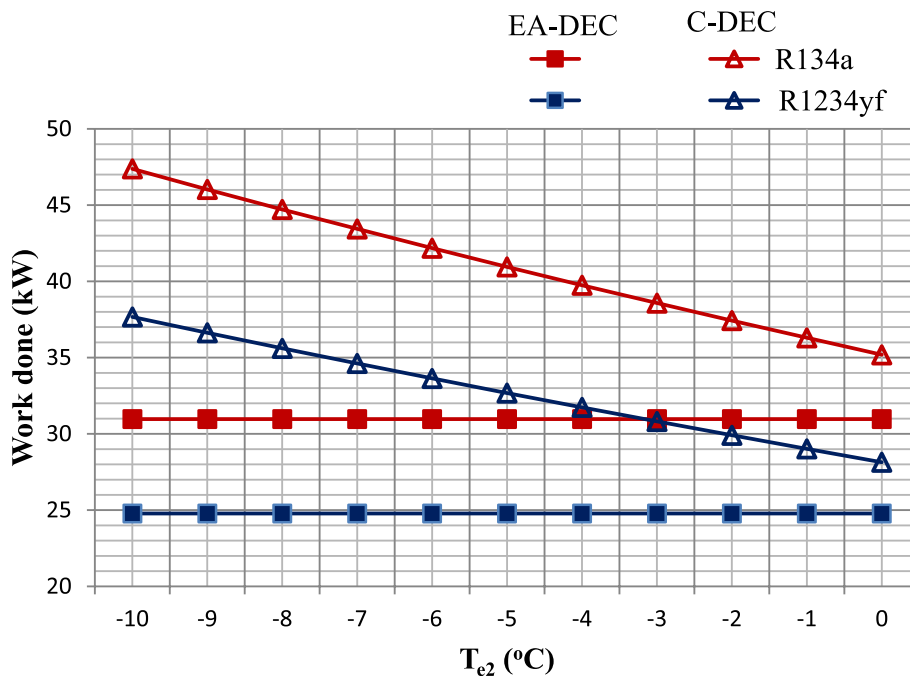


Fig. 14 Variation of compressor work with the evaporator-2 temperature

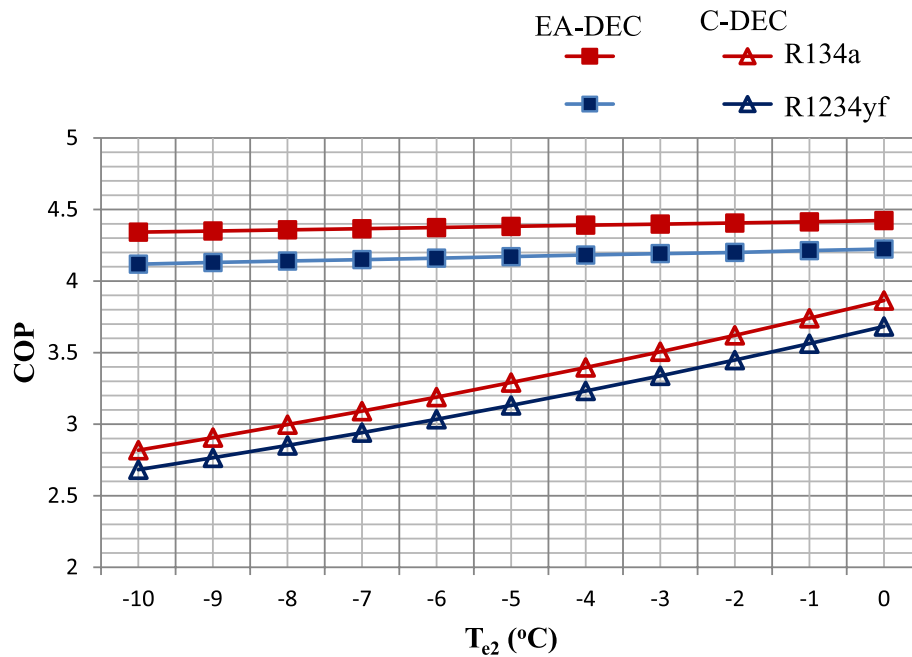


Fig. 15 Variation of COP with the evaporator-2 temperature

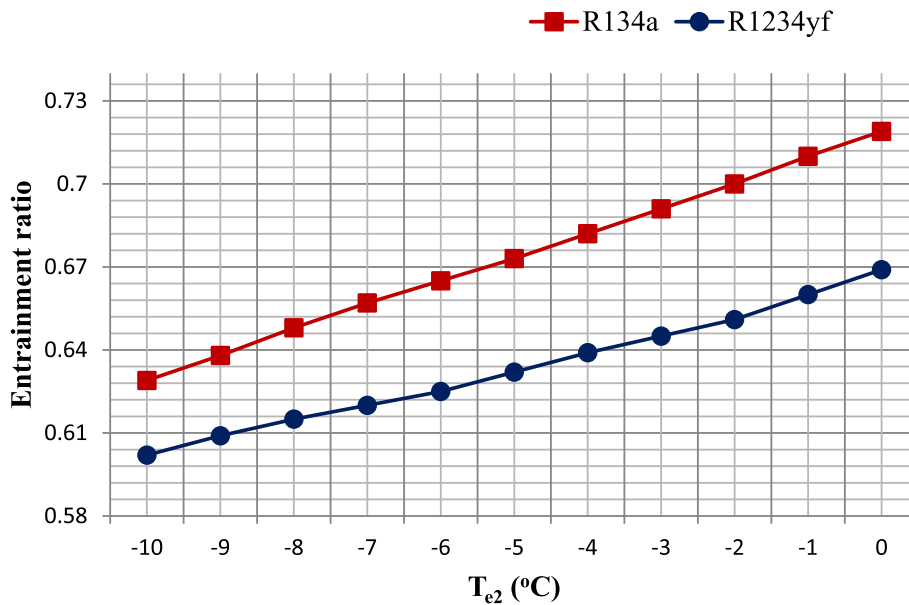


Fig. 16 Variation of entrainment ratio with the evaporator-2 temperature

3. With the increase in evaporator-1 temperature, refrigeration capacity of evaporator-1 increases, but it decreases for evaporator-2. However, the decrease in refrigeration capacity of evaporator-2 is negligible with R1234yf, but it is 5% with R134a. The total cooling capacity increases a little for both the cycles and refrigerants.
4. The compressor power of EA-DEC decreases with the increase in evaporator-1 temperature, but it remains almost constant for C-DEC. Therefore, the COP of EA-DEC increases considerably.
5. With the increase in evaporator-2 temperature, the refrigeration capacity of evaporator-1 decreases, but it increases for evaporator-2. The total refrigeration

capacity increases in both the cycles; however, the increase is more in the EA-DEC.

6. The compressor work of C-DEC reduces with the rise in evaporator-2 temperature, but it remains almost constant for EA-DEC. Therefore, the COP of C-DEC increases considerably.
7. The entrainment ratio improves with the rise in evaporator-2 temperature, but it reduces with the rise in evaporator-1 temperature.

7 Nomenclature

A: Cross-sectional area (m²)

C: Velocity (m/s)

COP: Coefficient of performance

h: Enthalpy (kJ/kg)

m: Mass flow rate (kg/s)

P: Pressure (kPa)

PLR: Pressure lift ratio

Q: Cooling capacity (kJ/kg)

s: Entropy (kJ/kg-K)

T: Temperature (°C)

W: Specific work (kJ/kg)

x: Vapor quality

Greek symbols

Δp : Pressure drop (kPa)

η : Efficiency

ρ : Density (kg/m³)

Φ : Area ratio

μ : Entrainment ratio

Subscripts

c: Condenser

comp: Compressor

d: Diffuser

e: Evaporator

imp: Improvement

is: Isentropic process

mix: Mixing section

p: Primary

pne: Primary nozzle exit

s: Secondary

sne: Secondary nozzle exit

1,2.....7: State points

Acknowledgements

This study is supported by the Device Development Program, Division of Department of Science & Technology, India, through grant no. DST/TDT/DDP-07/2017.

Authors' contributions

Gulshan Sachdeva: Conceptualization, Methodology, Resources, Writing, original draft, Supervision. Parinam Anuradha: Conceptualization, Formal analysis, Methodology, Project administration, Software, Supervision, Validation, Writing – review & editing. Vaibhav Jain: Methodology, Formal analysis, Software, Writing – review & editing. Y.T. VenkataTeja: Conceptualization, Formal analysis, Investigation, Resources, Software.

Availability of data and materials

The data that support the findings of this study are available from the corresponding author (V. Jain), upon reasonable request.

Declarations

Competing interests

The authors declare that they have no competing interests.

Received: 13 September 2023 Accepted: 17 February 2024

Published online: 19 March 2024

References

1. Kornhauser, A. A. (1990). The use of an ejector as a refrigerant expander. *International refrigeration and air conditioning conference. Paper, 82*, 10–19.
2. Sarkar, J., (2009). Performance characteristics of natural refrigerants based ejector expansion refrigeration cycles. *Proc IMechE J Power and Energy*, 223, 543–550.
3. Sarkar, J. (2010). Geometric parametric optimization of ejector expansion refrigeration cycle with natural refrigerants. *International Journal of Energy Resources*, 34, 84–94.
4. Li, H., Cao, F., Bu, X., Wang, L., & Wang, X. (2014). Performance characteristics of R1234yf ejector expansion refrigeration cycle. *Applied Energy*, 121, 96–103.
5. Gan, A., Klein, S., Reindl D., (2000). Analysis of refrigerator/freezer appliances having dual refrigeration cycles. *ASHRAE Transactions*, 106, 185–191.
6. Gang, Y., Cui, C., & Yu, J. (2015). Energy and exergy analysis of zeotropic mixture R290/R600a vapor-compression refrigeration cycle with separation condensation. *International Journal of Refrigeration*, 53, 155–162.
7. Hadi, R., Javad, R., Pouria, S. M., & Hadi, G. (2018). Novel dual loop bi-evaporator vapor compression refrigeration cycles for freezing and air-conditioning applications. *Applied Thermal Engineering*, 138, 563–582.
8. Cui, Z., Qian, S., & Yu, J. (2020). Performance assessment of an ejector enhanced dual temperature refrigeration cycle for domestic refrigerator application. *Applied Thermal Engineering*, 168, 114826.
9. Cui, L., Jia, Y., Yanzhong, L., Wenjian, C., Chen, L., & Haoran, C. (2016). Experimental study on a multi-evaporator refrigeration system with variable area ratio ejector. *Applied Thermal Engineering*, 102, 196–203.
10. Sarkar, J., (2010). Performance characteristics of multi-evaporator trans-critical CO₂ refrigeration cycles with hybrid compression/ejection. *Proc. IMechE 224 Part A: J. Power and Energy*, 224(6), 773–780.
11. Lawrence, N., Elbel, S. (2012). Experimental and analytical investigation of automotive ejector air conditioning cycles using low pressure refrigerants. *International Journal of Refrigeration Conference, July 16–19*. <http://docs.lib.purdue.edu/iracc>
12. Lawrence, N., & Elbel, S. (2013). Theoretical and practical comparison of two phase ejector refrigeration cycles including first law and second law analysis. *International Journal of Refrigeration*, 36, 1220–1232.
13. Lawrence, N., & Elbel, S. (2014). Experimental investigation of a two phase ejector cycle suitable for use with low pressure refrigerants R134a and R1234yf. *International Journal of Refrigeration*, 38, 310–322.
14. Latra, B., Haberschill, P., & Lallemeudo, A. (2014). Investigation of a novel-ejector expansion refrigeration system using the working fluid R134a and its potential substitute R1234yf. *International Journal of Refrigeration*, 45, 148–159.
15. Unal, S., & Yilmaz, T. (2015). Thermodynamic analysis of the two phase ejector air conditioning system for buses. *Applied Thermal Engineering*, 79, 108–116.
16. Unal, S. (2015). Determination of ejector dimensions of a bus air conditioning system using analytical and numerical methods. *Applied Thermal Engineering*, 90, 110–119.
17. Jeon, Y., Kim, S., Kim, D., Chung, H. J., & Kim, Y. (2017). Performance characteristics of an R600a household refrigeration cycle with a modified two phase ejector for various ejector geometries and operating conditions. *Applied Energy*, 205, 1059–1067.
18. Jeon, Y., Kim, D., Jung, J., Jang, D. S., & Kim, Y. (2018). Comparative performance evaluation of conventional and condenser outlet split

ejector based domestic refrigerator -freezers using R600a. *Energy*, 161, 1085–1095.

19. Gao, Y., Guogeng, H., Cai, D., & Fan, M. (2020). Performance evaluation of a modified R290 dual evaporator refrigeration cycle using two phase ejector as expansion device. *Energy*, 212, 118614.
20. Zilio, C., Brown, J. S., Schiochet, G., & Cavallini, A. (2011). The refrigerant R1234yf in air conditioning system. *Energy*, 36, 6110–6120.
21. Kim, S., Jeon, Y., Chung, H. J., & Kim, Y. (2018). Performance optimization of an R410A air-conditioner with a dual evaporator ejector cycle based on cooling seasonal performance factor. *Applied Thermal Engineering*, 131, 988–997.
22. Bilir, N., & Ersoy, H. K. (2009). Performance improvement of the vapour compression refrigeration cycle by a two-phase constant area ejector. *Int. J. of Energy Res.*, 33, 469–480.

Publisher's Note

Springer Nature remains neutral with regard to jurisdictional claims in published maps and institutional affiliations.